CHAPTER 16

NEMATIC ORDERED CELLULOSE: ITS STRUCTURE AND PROPERTIES

TETSUO KONDO*

Bio-Architecture Center (KBAC) and Graduate School of Bioresource and Bioenvironmental Sciences, Kyushu University, 6-10-1, Hakozaki, Higashi-ku, Fukuoka 812-8581, Japan

Abstract

The authors developed a unique form of β-glucan association, "nematic ordered cellulose" (NOC) that is molecularly ordered, yet noncrystalline. NOC has unique characteristics; in particular, its surface properties provide with a function of tracks or scaffolds for regulated movements and fiber production of *Acetobacter xylinum (=Gluconacetobacter xylinus)*, which produces cellulose ribbon-like nanofibers with 40–60 nm in width and moves due to the inverse force of the secretion of the fibers (Kondo et al. 2002). This review attempts to reveal the exclusive superstructure-property relationship in order to extend the usage of this nematic-ordered cellulose film as a functional template. In addition, this describes the other carbohydrate polymers with a variety of hierarchical nematic-ordered states at various scales, the so-called nano/micro hierarchical structures, which would allow development of new functional-ordered scaffolds.

Keywords

cellulose, hierarchical structure, nematic order, orientation, template.

1 INTRODUCTION

Interfacial surface structure and interaction of materials at the nanoscale have attracted much attention in the field of nanotechnology (Drexler 1992). Microbiological systems have been investigated as a microscale process (Zhao et al. 1998); however, recent studies showing the unique interaction of biological systems with entirely synthetic molecular assemblies have prompted

* For correspondence: Tel: +81-(0)92-642-2997; Fax: +81-(0)92-642-2997; e-mail: tekondo@agr.kyushu-u.ac.jp

R.M. Brown, Jr. and I.M. Saxena (eds.), Cellulose: Molecular and Structural Biology, 285–305.

consideration of a new generation of approaches for controlled nanoassembly (Whaley et al. 2000).

In biological systems, skeletal materials such as cell walls, bones, and shells are made primarily of a nanoscale building block of polysaccharides, proteins, and inorganic salts. The assembly of these building blocks facilitates the production of a hierarchical framework structure. Materials with hierarchical structures produced by organisms are mainly based on how the comprising components are biosynthesized and subsequently how they would be self-assembled. Once the structures are established, it is difficult to modify them into another form with a different function for an appropriate purpose.

In this sense, it is of importance in cellulose science including cell wall formation to understand various states on how molecules can be associated, and thereby how the higher hierarchical structure can be organized from molecular scales to micrometer scales through nanometer scales. In particular, interfacial surface structures and interactions are greatly important in fabrication of a hierarchical structure for 3D-materials built up from the molecules.

Cellulose comprises the major polymer of plant cell walls and has had a long history as a natural polymer material. The biomacromolecule, which is a β-1,4-glucan homopolymer, normally is classified according to how the β-glucan chains associate. We expand the concept how various states of molecular association can be categorized in cellulose. A major consideration is that the predominant crystalline state of cellulose is included as a component in the ordered state. This means that the ordered state also contains noncrystalline ordered states. The category "ordered" is in contrast to the "nonordered" state which to date has been considered as "amorphous cellulose" for lack of a useful way to characterize the product. It should be noted that in our concept, the amorphous state being categorized as the "nonordered" state, should be distinguished from the "noncrystalline" state of cellulose. Thus, in this classification, it becomes crucial whether the state is "ordered" or "nonordered." Namely, it may be advantageous to first prioritize whether or not the cellulose is in the ordered or nonordered domain, rather than determine if it is crystalline or noncrystalline. Figure 16-1 demonstrates the schematic representation of our concept. In this idea, a noncrystalline state in the ordered domain should have intermediates from amorphous to crystalline states, and these are important in determining further states of aggregation, which may lead to the crystalline state. Of course, the crystalline states are important, but so far, too much attention has been paid only for crystalline structures. A key concept here is that we should consider crystalline states as a subdivision of the broader concept of ordered domains.

Based on the above concept, we developed a new supramolecular associated form of glucan chains, nematic ordered cellulose (NOC), which is highly ordered, but not crystalline (Kondo et al. 2001). NOC has unique characteristics; in particular, its surface properties provide with a function of tracks or scaffolds for regulated movements due to the inverse force in production of nanocellulose fibers of *Acetobacter xylinum* (Kondo et al. 2002). When the

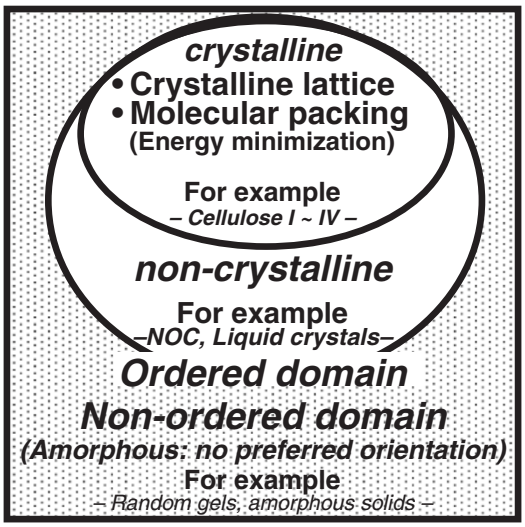

Figure 16-1. Our concept of glucan chain association for cellulose

interaction between the produced cellulose fibers called "bacteria cellulose ribbons" and specific sites of the oriented molecules on the unique surface of NOC is very strong, such ordered cellulose can be used as a template for the construction of nanocomposites, and the growth direction of the secreted cellulose is controlled by the epitaxial deposition of the microfibrils. Our proposed method is predicted to provide a novel type of nanotechnology using biological systems with molecular nanotemplates to design 3D-regulated structures. In order to extend the usage of this NOC film as a functional template, the present article will review the unique structure in relation to the exclusive surface properties of NOC, starting from how β-glucan association is initiated and established by uniaxial stretching of water swollen cellulose gel films (Kondo et al. 2004).

2 STRUCTURE OF NEMATIC ORDERED CELLULOSE

2.1 What is nematic ordered cellulose; NOC?

Prior to NOC, it will be required to know the characteristic feature of a cellulose molecule (Figure 16-2): cellulose owns an extended structure with a 2_1 screw axis composed by the β-1,4-glucosidic linkages between anhydroglucose units. Thus, it would be natural to accept the dimer called "cellobiose" as a repeating unit. The present three kinds of hydroxyl groups within an anhydroglucose unit exhibit different polarities, which contribute to formation of various kinds of inter- and intramolecular hydrogen bonds among secondary OH at the C-2,

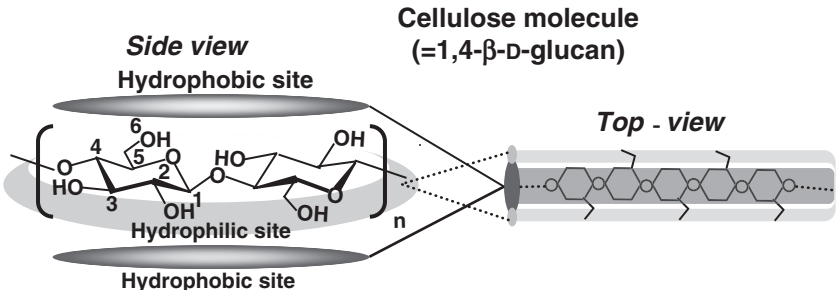

Figure 16-2. Site specific, amphiphilic nature in cellulose chemical structure

secondary OH at the C-3 and primary OH at the C-6 position. In addition, all the hydroxyl groups are bonded to a glucopyranose ring equatorially. This causes appearance of hydrophilic site parallel to the ring plane. On the contrary, the CH groups are bonded to a glucopyranose ring axially, causing hydrophobic site perpendicular to the ring as shown in Figure 16-2. These effects lead to formation of hydrogen bonds in parallel direction to a glucopyranose ring, and to Van der Waars interaction perpendicular to the ring.

Another important feature for the hydroxyl groups is the type of hydroxymethyl conformation at the C-6 position, because the conformation of C(5)–C(6) and the resulting interactions including inter- and intramolecular hydrogen bonds in the present cellulose structure may differ from that in crystallites and also it is assumed to make up the extent of crystallization, as well as the final morphology of cellulose. In the noncrystalline regions, the rotational position of hydroxymethyl groups at the C-6 position may be considered as indeterminate or totally nonoriented, which are not identical with those in the crystallites. Therefore, it was important to confirm the type of O(6) rotational position with respect to the O(5) and C(4) in a β-glucan chain, by employing CP/MAS ^{13}C NMR (Horii et al. 1983). The type of hydroxymethyl conformations is *gauche-trans* (***gt***), *trans-gauche* (***tg***), or *gauche- gauche* (***gg***) at the C-6 positions in carbohydrates. As for the noncrystalline states, they are considered as the *gg* conformation (see Figure 16-8).

Now, when the dissolved cellulose molecules are self-aggregated in water to form a gel presumably by a minimum amount of restricted engagements among hydrophobic sites of the ring above described, then it is stretched to reach NOC. Figure 16-3 illustrates structural characteristics of NOC in relation to the situation of OH groups explained in the following: NOC is prepared by uniaxial stretching of water-swollen cellulose from the *N*, *N*-dimethylacetamide (DMAc)/LiCl solution (the details are described in Section 5), and thereby, the cellulose molecular chains tend to be oriented toward the stretching axis (Togawa and Kondo 1999). Further, the hydroxymethyl groups at the C-6 position that are equatorial-bonded to the anhydroglucose unit are vertically stuck up against

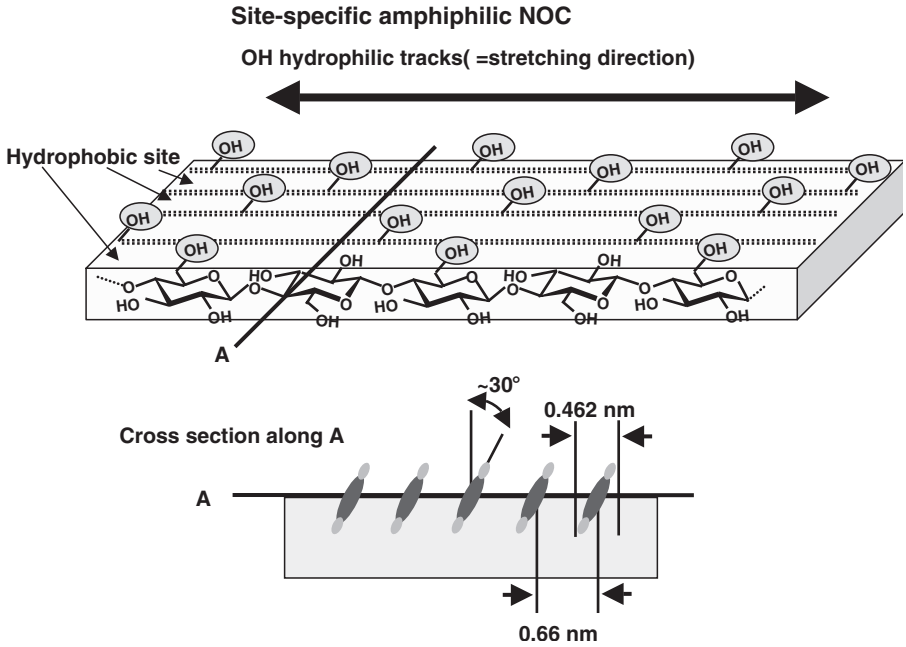

Figure 16-3. Schematic NOC surface structure and the cross section along the perpendicular A (=lateral direction) to the stretching direction

the surface, which indicates that the neighboring anhydroglucose ring planes are facing with each other. Simultaneously the stuck up OH groups in the individual molecular chains are also aligned like tracks along the stretching axis. On the contrary, the lateral order of the OH groups among the neighboring chains is not well coordinated because of the slipped molecular chain situation with each other. The uniaxial stretching also caused this situation. Therefore, the hydrophilic and polarized OH groups are totally to be oriented as molecular tracks only in the stretching direction across the entire NOC surface. Between the hydrophilic molecular tracks, the hydrophobic site due to the anhydroglucose plane was also appeared, resulting in both hydrophilic and hydrophobic tracks next to each other across the NOC surface. These amphiphilic molecular tracks enhance the unique surface properties of NOC as described later.

The NOC structure was basically indicated by the high-resolution transmission electron microscope (TEM) image. The NOC template with molecular ordering was shown in Figure 16-4 (Kondo et al. 2001). The high-resolution image obtained from the TEM shows a preferentially oriented direction on the surface. These observations confirmed the mean width of a single glucan chain corresponding to its known dimensions as viewed from its narrow axis of the anhydroglucose ring. The average chain width was 0.462 nm (standard

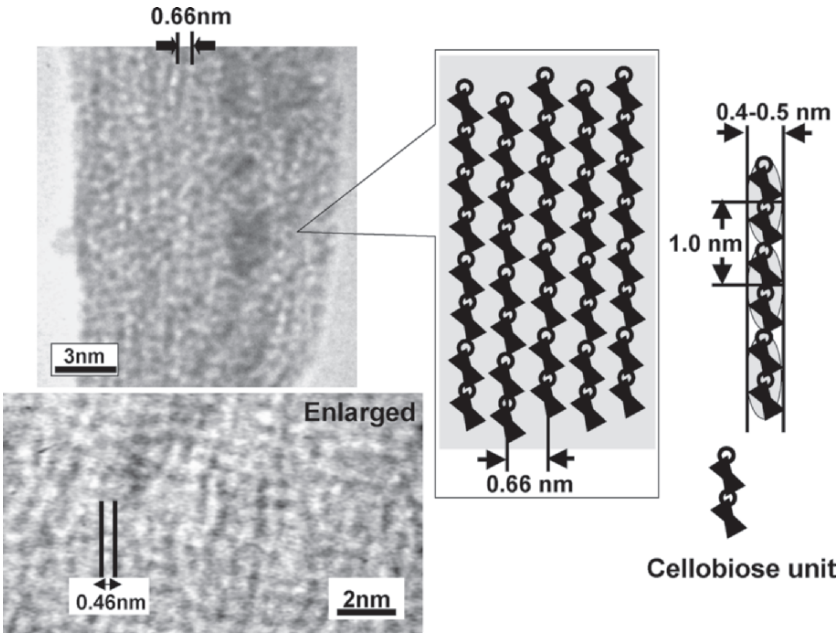

Figure 16-4. High-resolution TEM of NOC, the molecular ordering template (*left*). The film was negatively stained by uranyl acetate and spans a region of the copper support grid. Note the individual glucan chains that are separated by an average distance of 0.66 nm (*arrows*). In the enlarged image, the arrangement of glucan chains are clearly resolved with 0.46 nm in width. (*right*) Schematic diagram of NOC showing the arrangement of glucan chains and the linear spacing of the cellobiose units (*circled*). The polymer chains lie on their narrow axes

deviation = ±0.0517 nm). Thus, the true width seems to be ~0.4–0.5 nm when taking into account the negative stain. The average distance between two parallel chains was 0.660 nm (standard deviation = ±0.068 nm), which is wider than values for any crystalline cellulose. The average width of 0.462 nm from the top view is wider than that of 0.45 nm of the narrow axis in the anhydroglucose ring predicted from the space-filling model. This suggests tilting of the glucose planes of a cellulose molecule with a angle of 29.3° to the vertical axis against the surface of NOC as shown in the bottom image of Figure 16-3. It should be noted that the contact angle of a water drop of water on the NOC surface is ~72°, indicating fairly hydrophobic (Togawa and Kondo, unpublished). Prior to stretching for NOC preparation, the water-swollen cellulose exhibits ~50° as the contact angle. Thus, the surface condition of it is totally altered by stretching to provide tilting of the glucose planes for exposure of the specific hydrophobic site as shown in Figure 16-3.

The atomic force microscope (AFM) image analyses of the NOC surface without the negative stain demonstrate that well-aligned molecular aggregates

with a width of 4–6 nm and a height of ~6 nm in average are oriented uniaxially (Figure 16-5). The AFM resolution of the image is not at the molecular level. Without negative staining with uranyl acetate, it may be difficult to obtain a high resolution AFM image of the NOC surface, particularly the glucan chain images shown in the TEM micrograph of Figure 16-4, because of the surface flexibility when the AFM tip approaches close enough to observe the NOC surface.

The orientation parameter calculated from wide-angle x-ray diffraction (WAXD) photographs (Figure 16-6) became 0.88, which indicated a high degree of orientation. This means that the deviation (γ) anglę of molecular orientation to the stretching direction was $0.0° < \gamma < 10.5°$. However under these conditions, the crystallinity did not significantly follow the increase of the orientation by the stretching (Togawa and Kondo 1999). Simultaneous orientation and crystallization did not occur as often seen with crystalline polymers (Ward 1997). The crystallinity was ~14.8 and 16.8% before and after stretching, respectively. Infrared spectra of deuterated samples also supported a low crystallinity of the film based on the ratio of the remaining hydroxyl groups in the drawn films that corresponds to the crystallinity index.

Figure 16-6 shows wide-angle x-ray diffraction (WAXD) intensity curves in both equatorial and meridional directions of NOC together with cellulose II fibers. In the equatorial diffraction of NOC, typical crystalline diffraction patterns representing cellulose II (Figure 16-6a) were not observed. The diffuse intensity equatorial profile for NOC (Figure 16-6b) indicated that it contains considerably more "amorphous" regions. The meridional scan of WAXD was employed to analyze the order along the stretching direction for NOC. Meridional intensities of cellulose are affected by the disorder of the neighboring chains that is symmetrical for the chain axis. In general, cellulose polymorphs provide almost the same meridional patterns; namely two strong distinct reflections of the (002) and (004) planes ($2\theta = 17.2°$, $d = 0.516$ nm; $2\theta = 34.7°$, $d = 0.259$ nm, respectively; see the right of Figure 16-6a).

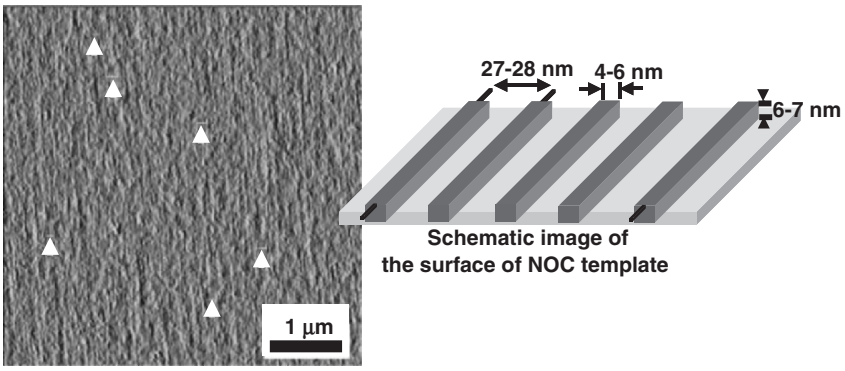

Figure 16-5. Atomic force micrographs showing the surface of the nematic ordered cellulose (NOC) template with a schematic representation

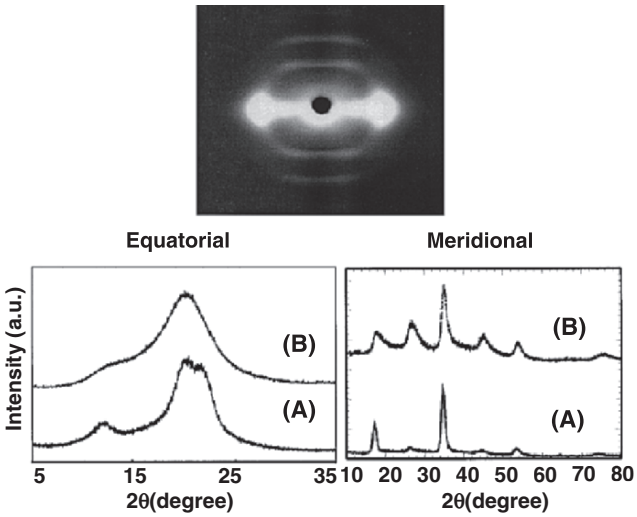

Figure 16-6. WAXD photograph of NOC together with equatorial (*left*) and meridional (*right*) intensity curves of the WAXD for cellulose II fibers (**a**) and NOC (**b**). The term, "a.u." indicates arbitrary unit

The present results demonstrate that NOC, which is highly ordered but noncrystalline, gives a totally different profile for the meridional scan as shown in Figure 16-6b. More reflections were found in the meridional direction when compared with cellulose II crystals. The characteristics are considerable line broadening of the meridional reflections in the profile of NOC. This indicates that the structure of the NOC film along the chain direction may have a certain disorder that causes the ordered, but noncrystalline regions. It may be considered that the situation is not a perfect disorder in the molecular chain direction, but some registrations may exist. Considering the crystallinity of the film sample (16.8%), the meridional direction profile should contain the contribution due to cellulose II crystals. When the contribution of the crystallite is subtracted from the meridional direction profile in Figure 16-6b, each reflection in the same figure would tend to have the similar shape and intensity as shown in Figure 16-7. Thus, we should consider the states of the structure for NOC to be ordered states that are neither crystalline nor amorphous.

Parallel to the x-ray diffraction, NOC also exhibited a diffuse pattern in the TEM electron diffraction mode, similar to that from x-ray diffraction of Figure 16-6 (not shown here).

As already described, the type of hydroxymethyl conformation at the C-6 position is assumed to provide the extent of crystallization, as well as the final morphology of cellulose (Horii et al. 1983; Kondo and Sawatari 1996; Togawa and Kondo 1999). The conformation of C(5)–C(6) and the resulting interactions including hydrogen bonds in NOC differ from that in crystallites.

CP/MAS ^{13}C NMR may suggest the type of hydroxymethyl conformations, ***gt***, ***tg***, or ***gg*** at the C-6 positions in carbohydrates as shown in Figure 16-8. Horii

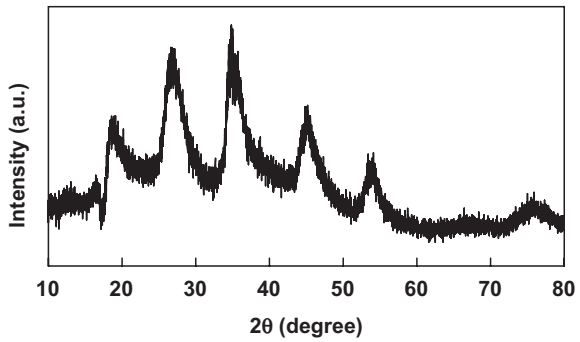

Figure 16-7. Calibrated meridional intensity curve of the WAXD for NOC. The term, "a.u." indicates arbitrary unit

et al. (1983) indicated that C-6 carbon resonance occurs only as a singlet near 64 ppm in the case of the *gt* conformation whereas a resonance band near 66 ppm appears when the ***tg*** conformation is present within the crystalline structures. According to these researchers, the chemical shifts fall into three groups of 60–62.6, 62.5–64.5, and 65.5–66.5 ppm, which are related to ***gg***, ***gt***, and ***tg*** conformations, respectively. The chemical shift of the C-6 for cellulose II (Dudley et al. 1983; Horii et al. 1985; Isogai et al. 1989) indicated the ***gt*** conformation,

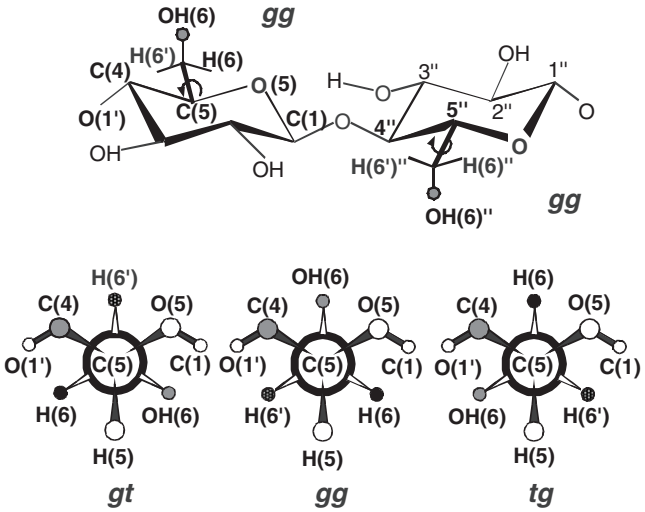

Figure 16-8. Schematic diagram of the hydroxymethyl conformations at the C-6 position, namely the orientation of the C6–O6 bond, *gauche-trans* (***gt***), *trans-gauche* (***tg***) or *gauche-gauche* (***gg***) with a cellobiose unit

which may agree with recent results from the neutron fiber diffraction analysis (Langan et al. 1999). As for the noncrystalline states, they are considered in the *gg* conformation. Therefore, it is easy to predict that NOC could have ***gg*** conformation of the hydroxymethyl group at the C(6) position.

In Figure 16-9, the CP/MAS ^{13}C NMR spectra for our NOC sample, as well as amorphous (a noncrystalline state without any preferred orientation) cellulose prepared from cellulose-SO_2-dimethylamine-dimethyl sulfoxide solution (Isogai and Atalla 1991) and CF11 cellulose powder (Whatman International Ltd.) are shown in the range from 50 to 80 ppm where chemical shifts at the C (6) position appear.

The chemical shift of CF11 appears at 65 ppm, corresponding to ***tg*** conformation, indicating that CF11 is native cellulose. Our NOC sample exhibits a broader signal similar to amorphous cellulose within the range of the type of the hydroxymethyl conformation, ***gg***, which also supports our suggestion that NOC is noncrystalline even though it is well ordered.

2.2 Nematic ordered α-chitin and cellulose/α-chitin blends

2.2.1 Nematic ordered α-chitin

Figure 16-10 shows high-resolution TEM(CHRTEM) images of molecular assembly in the stretched samples of α-chitin and cellulose/α-chitin blend with a composition of 25/75 that were prepared by the same manner for NOC and subsequently negatively stained with uranium acetate. They exhibited occurrence of the orientation of molecular aggregation as seen in white lines, but were not resolved at the individual molecular chain scale, unlike the high-resolution TEM image of NOC (Kondo et al. 2001). By image analyses of the two TEM

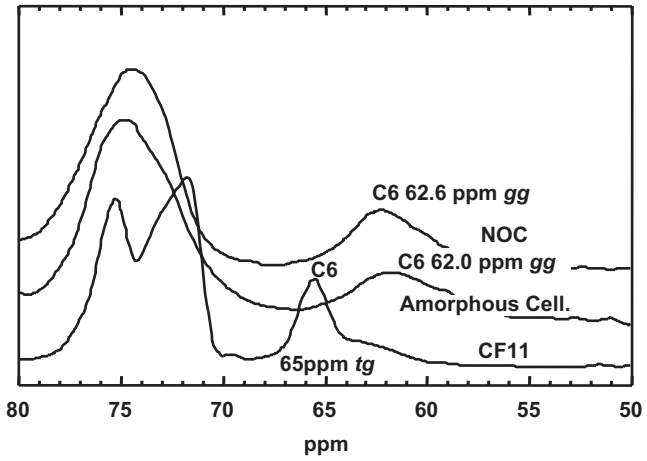

Figure 16-9. CP/MAS ^{13}C NMR spectra of NOC, amorphous cellulose, and native cellulose powder (Whatman CF11)

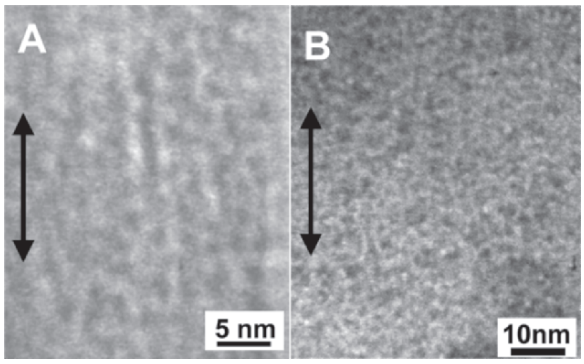

Figure 16-10. HRTEM images of single molecular chains in the order structure of the stretched water-swollen gel films at the drawing ratio of 2.0 of (**a**) α-chitin and (**b**) cellulose/α-chitin (25/75) blend. The double arrows indicate the stretching direction

photographs in Figure 16-10, the average width and distance between two parallel lines were obtained as listed in Table 16-1 in comparison of NOC data.

The crystal lattice parameters for native crystalline α-chitin were reported as $a = 0.474$ nm, $b = 1.886$ nm, $c = 1.032$ nm, and $\alpha = \beta = \gamma = 90°$, respectively (Minke and Blackwell 1978). Since the average distance between any two lines in well-ordered states in Figure 16-10a was 1.88 ± 0.27 nm, this value coincides with the lattice dimension of *b*-axis. Therefore, considering that the stretching direction corresponds to the molecular chain axis (*c*-axis), the top view of the TEM image of Figure 16-10a indicates that the b-c plane of α-chitin microfibril may be aligned parallel as white lines with a distance of 1.62 ± 0.21 nm on the surface. In other words, by the same preparation method for NOC, α-chitin molecules may be self-assembled to form a microfibril, and further the individual microfibrils tend to be arranged parallel with the distance of 1.62 ± 0.21 nm. This indicates presence of another nematic ordered state with a different scale in α-chitin.

2.2.2 Nematic ordered cellulose/α-chitin blends

Figure 16-10b and the corresponding data in Table 16-1 exhibit a case of the stretched film of the cellulose/α-chitin blend with a composition of 75/25 (w/w) in the same manner for NOC.

Table 16-1. The average width and distance between two parallel lines analyzed by TEM images

			(nm)
	Cellulose (NOC)*	α-Chitin	Cellulose/α-Chitin 75/25
Line width	0.46 ± 0.05 (chain width)	1.88 ± 0.27	1.38 ± 0.18
Distance between two lines	0.66 ± 0.07	1.62 ± 0.21	1.65 ± 0.27

*From Kondo et al. (2001).

The white dots or lines in Figure 16-10b indicate molecular chains or molecular aggregates. Some parts are well oriented parallel to the stretching direction, and the molecular aggregates are entirely ordered along the stretching axis. The average line width as shown in Table 16-1 is narrower than that for nematic ordered pure α-chitin, indicating that the intermolecular interaction between cellulose and α-chitin may be engaged. Possibly each molecular chain is facing with each other against the surface by a hydrophobic interaction such as a van der Waals force. On the other hand, the average distance between two parallel lines was not significantly different between the two stretched films from α-chitin and the cellulose/α-chitin blend. Therefore, it is considered that the cellulose/α-chitin molecular aggregates in the stretched film are aligned similarly to nematic ordered α-chitin.

To deal with the above case in comparison of the NOC, we employed WAXD measurements in order to understand the molecular ordering occurring during stretching of the blended films of the water swollen cellulose/α-chitin (50/50) gel. Water-swollen gel-like cellulose films formed after slow coagulation and the subsequent solvent-exchange were transparent and composed of ~93 wt% of water and 7 wt% of cellulose prior to stretching. When stretching the water-swollen film uniaxially, drops of water extruded from the film as the orientation of the film increased. The films stretched at the changing drawing ratio were provided for WAXD measurements.

Figure 16-11 shows WAXD photographs of the fiber structure. It suggests that the undrawn cellulose films after dried in a stretching device showed some orientation by natural shrinking, and with increase in drawing ratio of the samples, the rings were becoming arcs at the equatorial direction. Figure 16-12 shows WAXD photographs for the stretched cellulose/α-chitin (50/50) films at the desired drawn ratio.

When compared with that for cellulose shown in Figure 16-11, clearer Debye rings appeared even in undrawn films after dried. Like the cellulose case, with increase in drawing ratio of the samples, the rings were becoming arcs at the equatorial direction. Similarly, such arcs appeared also at the meridional direction. WAXD intensity curves in both directions indicate more clearly that some ordered crystallites, to some extent, were formed prior to stretching (data not shown, see Kondo et al. 2004). Through the stretching, the two peaks at $2\theta = 9.3$ and 19.5 in the equatorial direction were becoming narrower and sharper, while the meridional reflections were not significantly changed after the stretching. These results indicate that the intermolecular interaction between cellulose and α-chitin may cause molecular aggregations leading to some crystallization, and as a result, crystallites with a certain size were formed. Then, by stretching, the crystallites tend to be ordered parallel to the drawing axis.

The series of α-chitin used as a component for preparation of nematic ordered states have indicated that unlike NOC, at first the molecules tend to be aggregated prior to stretching, and then by the stretching the nematic ordered states of the aggregates were formed (Kondo et al. 2004). Namely, the nano/micro-hierarchical structures are supposed to be built up.

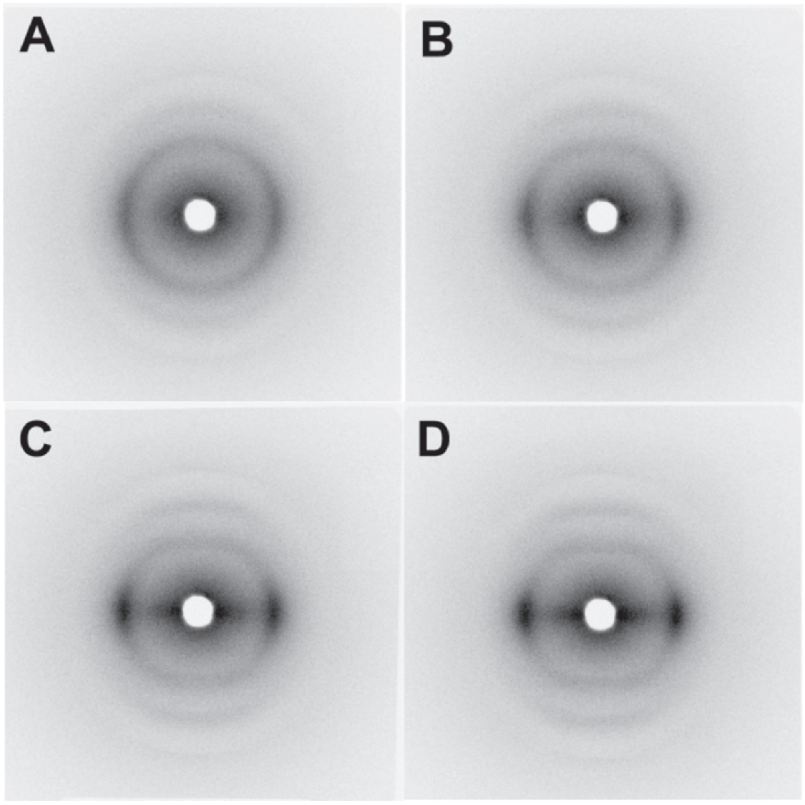

Figure 16-11. WAXD photographs for stretched cellulose films at the desired drawn ratio: (**a**) undrawn water-swollen film after dried at a fixed state; (**b**) draw ratio 1.5; (**c**) draw ratio 1.7, and (**d**) draw ratio 2.0

2.3 Another type of nematic ordered cellulose: honeycomb-patterned cellulose

Recently, a honeycomb-patterned cellulose triacetate film was successfully fabricated by casting of water-in-oil (W/O) emulsion on the substrate, and the subsequent deacetylation yielded a honeycomb-patterned cellulose film without deformation as shown in Figure 16-13 (Kasai and Kondo 2004). In the film forming process, when cellulose triacetate started to be precipitated as a honeycomb-patterned film, the honeycomb frames were supposed to be simultaneously stretched by natural drying of water droplets as a mold. This stretching effect of natural dry presumably resulted in an alignment of cellulose molecular chains along the honeycomb frames, similarly to formation of NOC-typed form (Kasai et al., unpublished).

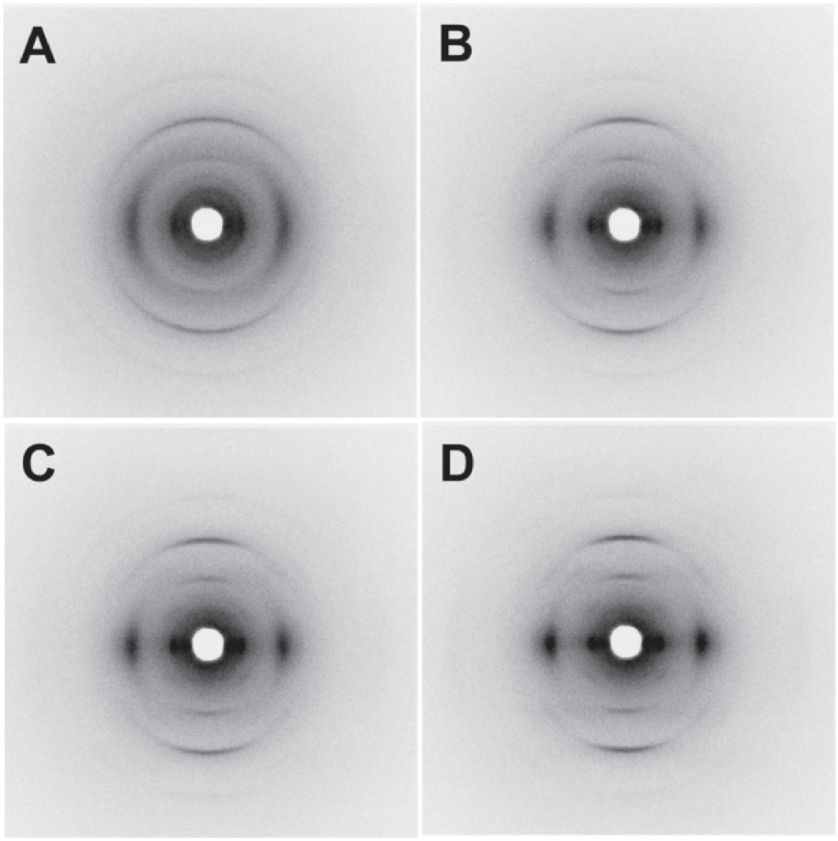

Figure 16-12. WAXD photographs for stretched cellulose/α-chitin (50/50) blended films at the desired drawn ratio: (**a**) undrawn water-swollen film after dried at a fixed state; (**b**) draw ratio 1.5; (**c**) draw ratio 1.7; and (**d**) draw ratio 2.0

3 PROPERTIES OF NEMATIC ORDERED CELLULOSE

3.1 The exclusive surface property of NOC and its unique application

As already described, NOC is considered as the template having the exclusive surface of a certain nano/micro structure. Namely, the OH groups together with the neighboring hydrophobic sites tend to be oriented as molecular tracks only in one direction across the entire NOC surface. These amphiphilic ordering tracks on the NOC surface were expected to induce an epitaxial deposition of substances such as organic and inorganic compounds. This is a unique application of NOC with a specific surface property to induce other substances to be oriented.

The ordering amphiphilic tracks of hydrophilic OH groups and hydrophobic polarity in NOC, for example, could induce an epitaxial deposition of biosynthesized

cellulose nanofibers secreted from the gram-negative bacterium, *A. xylinum* (=*Gluconacetobacter xylinus*), along the same axis of the tracks in NOC (Kondo et al. 2002). When active *A. xylinum* cells are transferred to the oriented surface, they synthesize cellulose ribbons parallel to the molecular orientation of the substrate. This is evidenced by direct video imaging of the motion of the bacteria as they synthesize the cellulose ribbon. The movement of *A. xylinum* in relation to cellulose biosynthesis was reported (Brown, Jr. et al. 1976). The cell movement (at a constant rate of 4.5 μm/min at 24°C) is the result of an inverse force imposed by the directed polymerization and crystallization of the cellulose. It is also well known that the bacterium rotates on its own axis.

This bio-directed epitaxial nanodeposition can be studied over time and under varied conditions including different substrates. For example, in Figure 16-14, a time-course analysis of an NOC template shows a bacterium moving in contact with a stretched NOC substrate.

Midway through this series, the cell, "jumps off" of the oriented substrate, and continues to secrete its cellulose ribbon but now in the form of a spiral that is the normal pattern of formation when not in contact with any organized substrate (Thompson et al. 1988). When the interaction between the bacterium and the surface of NOC is strong enough, the bacterium follows the track of the molecular template. As the polymer orientation of the NOC is not necessarily perfect, the bacterium may jump off the track at a structural defect (Figure 16-14 stage 3). After the bacterium leaves the track (Figure 16-14 stages 3–6), two forces, the inverse force of the secretion and the close interaction of adjacent microfibrils, affect the bacterium, possibly resulting in the synthesis of a spiral ribbon of microfibrils. In addition, the bacterium begins to rotate on its own axis. This rotation is the visible result of ribbon twisting which occurs to relieve strain induced by the absence of interaction with the substrate. When the ribbon is assembled in direct contact

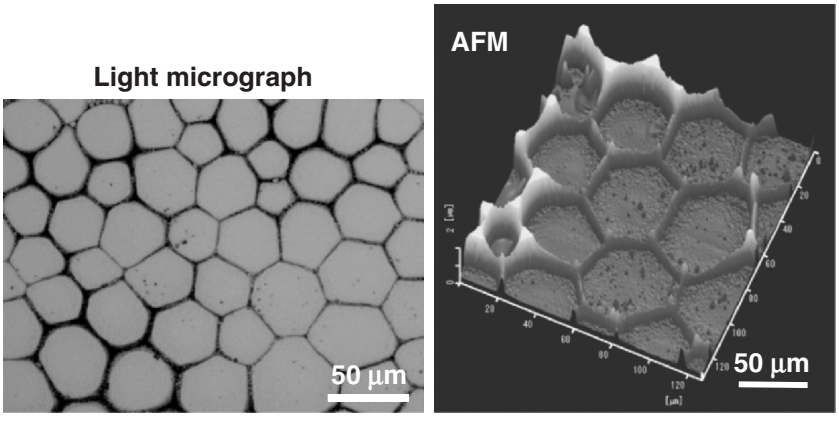

Figure 16-13. Light micrograph of honeycomb-patterned cellulose films from cellulose triacetate together with the surface topographic AFM image. (Scale bars are 50 μm.)

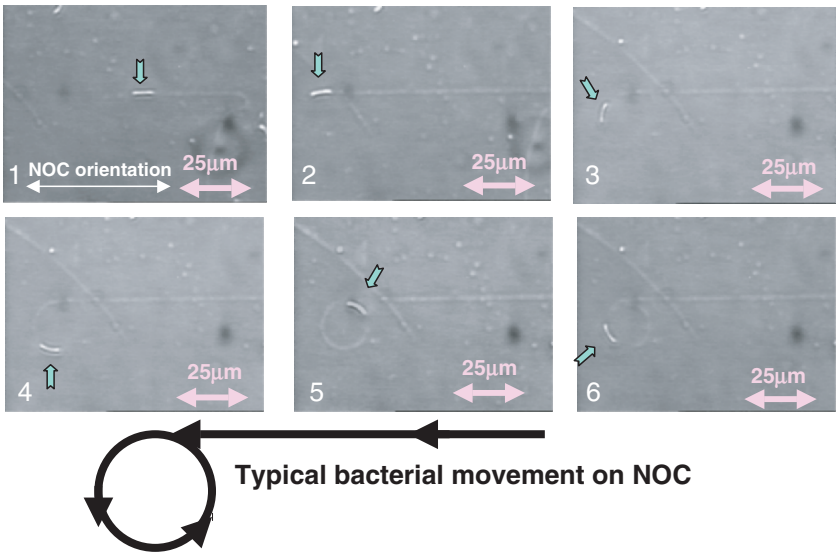

Figure 16-14. Successive images showing the motion of a bacterium as it secretes a cellulose ribbon using real-time video analysis. In (1), the bacterium is attached to and synthesizing its cellulose on the monomolecular rail track. In (2), the bacterium has jumped the track and is beginning to change its orientation. (3) to (5), the bacterium is generating the first complete spiral. In (6), the bacterium is on the second rotation of a spiral

with the oriented molecular NOC substrate, ribbon twisting is prevented, thus suggesting a control of this oriented solid surface over the final physical interaction of polymer chains immediately after synthesis and during the early stages of crystallization.

Cellulose ribbon interaction is more clearly shown by field emission scanning electron microscopy (FE-SEM) in Figure 16-15. In this experiment, the motion of the same sample is observed using light microscopy and then the sample is prepared for FE-SEM observations. In Figure 16-14 stage 1–2, the time-course sequence demonstrates an intense, directed nanodeposition that is exclusively linear and without cell rotation as the bacterium follows the track. This is confirmed by the ribbon structure shown by the FE-SEM images in Figure 16-15, a–c which reveal no twisting and a more perfect alignment with the substrate. Likewise, when the bacterium "jumps off" the track, the cellulose ribbon is twisted. On the other hand, when *Acetobacter* is cultured on the surface of a nonstretched cellulose swollen gel substrate (precursor for NOC), it moves in a random manner including spirals (data not shown). An FE-SEM image on the nonoriented substrate is shown in Figure 16-15e. The image suggests a random of microfibrils with the substrate surface. When *Acetobacter* cells are placed on an agar surface as a control, their interaction seems to be reduced, and twisted ribbons are always deposited, also in a random fashion (Figure 16-15f). It should be noted that this regulated movement of the bacterium was not observed in the synthetic polymers

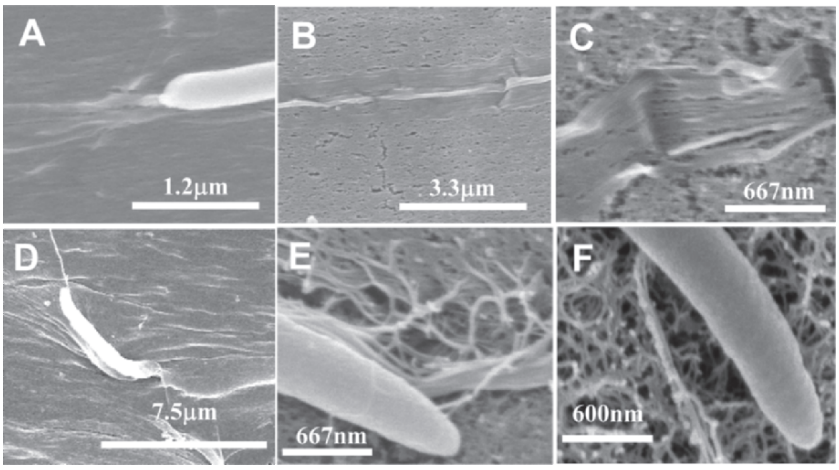

Figure 16-15. FE-SEM images of the cellulose ribbon deposition process. (**a**–**c**) examples of bacteria synthesizing cellulose ribbons on the oriented molecular track of NOC. In 15A, a bacterium shows a flat ribbon immediately behind its site of synthesis. (**b**) and (**c**) demonstrate the tight association between the molecular track and the cellulose ribbon. (**d**) is an example where the bacterium has just jumped off the track and following a spiral path. (**e**) demonstrates random cellulose deposition on the surface of a nonstretched NOC precursor. (**f**) shows random cellulose deposition on the surface of agar

having OH groups such as poly (vinyl alcohol), but only in nematic ordered states of carbohydrate polymers (Kondo et al. 2002). The authors have been recently successful to have the bacterium followed on the honeycomb-patterned cellulose frame having NOC states, resulting in 3D honeycomb cellulose structure (Kasai et al. unpublished).

The rate and direction of the movement correspond to those of the fiber production. The fibers were reported to produce at a rate of 2 μm/min at 25°C (Brown, Jr. et al. 1976). However, *A. xylinum* produced the fiber faster on NOC templates at a rate of 4.5 μm/min at 24 °C. This gap was considered due to difference of the strength of the interaction between the biosynthesized fiber and the NOC surface. This also indicated that the NOC surface promoted the secretion rate of the fibers. More to importance, the regulated movement of the bacteria due to the ordered surface of NOC may trigger the development a 3D structure of hierarchical architecture from the nano to the microlevels. Therefore, we have been attempting to regulate the 3D architecture of materials using the nanofibers secreted by *A. xylinum* as a building block.

4 THE FUTURE

In biological systems, skeletal materials such as cell walls, bones, and shells are made primarily of a nanoscale building block of polysaccharides, proteins, and inorganic salts. The assembly of these building blocks facilitates the production

of a hierarchical framework structure. The formation dynamics observed in this study could be applicable to the design of nanoscale controlled, hierarchically structured materials with specific properties. We have employed a biological system combined with a polymer platform having NOC-like surface in order to directly fabricate hierarchically ordered materials from the nanolevel up to the micron level. Therefore, such a surface property would greatly extend the possibilities of usage of cellulose to new areas. Thus, if a micropatterned film having a similar characteristic as NOC can be fabricated, the obtained 3D cellulose materials will be widely appreciated and used.

5 MATERIALS AND METHODS

5.1 Materials

Bleached cotton linters with a degree of polymerization (DP) of 1,300 were used as the starting cellulose sample. The cellulose was first dried under vacuum at 40°C. *N*,*N*-dimethylacetamide (DMAc) purchased from Katayama Chemicals Co. Ltd. (99+%) was dehydrated with molecular sieve 3A and used without further purification. Lithium chloride (LiCl) powder (Katayama Chemicals Co. Ltd.) was oven-dried at least for 3 days at 105°C. Methylcellulose with a degree of substitution (DS) of 1.6 and polyvinyl alcohol (PVA) with a DP of 2,000 were purchased from Shin-Etsu Chemical Co. Ltd. and Katayama Chemicals Co. Ltd., respectively. Cellulose acetate with a DS of 2.45 (L-70) and purified chitin were provided by Daicel Chemicals Co. Ltd. and Katakura Chikkarin, respectively.

NOC was prepared by stretching a water-swollen cellulose film which had been coagulated from a DMAc /LiCl solution. Dissolution of cellulose and preparation of the template was accomplished by a previously described procedure using a solvent exchange technique (Togawa and Kondo 1999).

5.2 Water-swollen cellulose film from the DMAc/LiCl solution

LiCl dried at 105°C was dissolved in anhydrous DMAc to give a concentration of 5% (w/w) solution. Dissolution of cellulose was basically followed by a previous swelling procedure using a solvent exchange technique (Togawa and Kondo 1999). Prior to swelling, the cellulose sample was disintegrated into fragments or small pieces by a mechanical disintegrator and dispersed into water which increased the surface area making it easier to dissolve. The treated cellulose was soaked in water overnight, then squeezed and filtered to remove the water. The cellulose was then immersed in methanol, and again squeezed and filtered to remove excess methanol. After four repetitions of the methanol treatments, an exchange with acetone was performed once. Following the treatments with water, methanol, and acetone described above, the sample was solvent-exchanged with DMAc twice in the same procedure and soaked in the same solvent overnight.

Another two repetitions of the above soaking and squeezing treatments with DMAc treatments were performed on the sample. Following the final squeeze, the cellulose was ready to be dissolved. The cellulose swollen by DMAc was dissolved in the DMAc/LiCl solution with constant stirring at room temperature for 3 weeks at most. As the viscosity of the solution depends on the DP of the polymer, ~1% cellulose with a DP of 1,300 was suitable for handling. After a week, when no change in viscosity was noted in the solution, 1–3% LiCl was added to the solution, and then it was heated up to 50–60°C for several hours. The resulting solution was then centrifuged and filtered to remove any insoluble portion. The actual concentration (wt%) of cellulose in the solution was determined by weighing a small portion of the dried cellulose film. At this stage, the molecules are almost completely dispersed.

The slow coagulation to prepare the gel-like film from a DMAc/LiCl solution was carried out according to the following manner. The solution was poured into a surface-cleaned glass Petri dish with a flat bottom and placed in a closed box containing saturated water vapor at room temperature. In this manner, saturated water vapor slowly diffused into the solution and precipitated the cellulose. The sample was allowed to stand at room temperature for several days until the precipitation under a saturated water vapor atmosphere was sufficiently complete to obtain the gel-like film. The precipitated gel-like film was washed with running distilled water for several days to remove the solvent, and a water-swollen transparent gel-like film was obtained. The films were stored in water until needed. It should be also noted that in the entire procedure from preparation of the solution until starting the slow coagulation with water vapor, rapid operation was required, otherwise the water vapor in the atmosphere would easily penetrate into the solution and cause precipitation of cellulose II crystals.

5.3 Preparation of NOC from water-swollen cellulose films

Drawn cellulose films were prepared by stretching water-swollen gel-like films. These films were cut into strips ~30 mm long and ~5 mm wide. These water-swollen strips then were clamped in a manual stretching device and elongated uniaxially to a draw ratio of 2.0 at room temperature. As the water-swollen films were gel-like, they could neither be clamped too tightly nor too loosely in the first stage of stretching. The entire drawing process was completed while the specimen was still in a wet state. Following air-drying, the drawn specimen in the stretching device was vacuum-dried at 40–50°C for more than 24 hours. The thickness of the dried films was about 80 μm.

5.4 Preparation of NOC template in Schramm-Hestrin (SH) medium

The never-dried NOC template was put into Schramm-Hestrin (SH) medium (Hestrin and Schramm 1954) at pH 6.0, and the solvent was exchanged and finally maintained in a Petri dish until used for the study.

Other noncrystalline ordered substrates were prepared in the same manner from different polymers. Nematic ordered blend films of cellulose and its derivatives were prepared as follows: DMAc/LiCl was used as the common solvent for all samples to be mixed. Solution concentrations were 1 wt% for cellulose and 5 wt% for the cellulose derivatives. All solutions were filtered and stored in a closed container. Separately prepared solutions of the cellulose and its derivatives were mixed at room temperature in the desired proportions. The relative composition of the two polymers in the mixed solutions was 70/30, 50/50, and 30/70 by weight (cellulose/the derivatives). After stirring for more than 3 days, the mixed solutions were used to prepare nematic ordered blend films by coagulation. The slow coagulation to prepare the gel-like film from a DMAc/LiCl solution was carried out according to the above. The solution was poured into a surface-cleaned glass Petri dish with a flat bottom and placed in a closed box containing saturated ethanol vapor at room temperature. In the blend solution, saturated ethanol vapor slowly diffusing into the solution was employed to precipitate the cellulose/cellulose derivative blend gel, instead of water vapor for NOC. It was allowed to stand at room temperature for a few days until precipitation under a saturated ethanol vapor atmosphere was complete to obtain the gel-like film. The precipitated gel-like film (at this stage fixation of the film appeared to be complete) was washed thoroughly with ethanol to remove the solvent, and then the film was put in water to exchange the solvent in order to obtain a water-swollen transparent gel-like film. This water-swollen cellulose/the derivative blended film was stretched in the same manner for NOC to be formed into nematic ordered blended films.

Acknowledgments

The author thanks Professor R.M. Brown, Jr. at University of Texas, Austin for the research collaboration and his valuable comment. Mr. Togawa and Ms. Hishrikawa at FFPRI are acknowledged by the long-term research collaboration. Dr. W. Kasai and Ms. Y. Tomita in my laboratory at Kyushu University are also acknowledged by their valuable comment on the text. This research was supported partly by a Grant-in-Aid for Scientific Research (No. 14360101), Japan Society for the Promotion of Science (JSPS).

REFERENCES

Brown, Jr. R.M., Willison J.H.M., and Richardson C.L. 1976. Cellulose biosynthesis in *Acetobacter xylinum*: visualization of the site of synthesis and direct measurement of the *in vivo* process. Proc Natl Acad Sci USA 73:4565–4569.

Drexler K.E. 1992. Nanosystems: Molecular Machinery, Manufacturing, and Computation. Wiley, Interscience, New York.

Dudley R.L., Fyfe C.A., Stephenson P.J., Deslandes Y., Hamer G.K., and Marchessault R.H. 1983. High-resolution carbon-13 CP/MAS NMR spectra of solid cellulose oligomers and the structure of cellulose II. J Am Chem Soc 105:2469–2472.

Hestrin S. and Schramm M. 1954. Synthesis of cellulose by *Acetobacter xylinum*. 2. Preparation of freeze-dried cells capable of polymerizing glucose to cellulose. Biochem J 58:345–352.

Horii F., Hirai A., and Kitamaru R. 1983. Solid-state ^{13}C-NMR study of conformations of oligosaccharides and cellulose conformation of CH_2OH group about the exo-cyclic C–C bond. Polym Bull 10:357–361.

Horii F., Hirai A., Kitamaru R., and Sakurada I. 1985. Cell Chem Technol 19:513.

Isogai A. and Atalla R.H. 1991. Amorphous celluloses stable in aqueous media: regeneration from SO_2-amine solvent systems. J Polym Sci Polym Chem 29:113–119.

Isogai A., Usuda M., Kato T., Uryu T., and Atalla R.H. 1989. Solid-state CP/MAS carbon-13 NMR study of cellulose polymorphs. Macromolecules 22:3168–3173.

Kasai W. and Kondo T. 2004. Fabrication of honeycomb-patterned cellulose films. Macromol Biosci 4:17–21.

Kasai W., Morita M., and Kondo T. unpublished.

Kondo T. and Sawatari C. 1996. A Fourier transform infra-red spectroscopic analysis of the character of hydrogen bonds in amorphous cellulose. Polymer 37:393–399.

Kondo T., Togawa E., and Brown, Jr. R.M. 2001. "Nematic ordered cellulose": a concept of glucan chain association. Biomacromolecules 2:1324–1330.

Kondo T., Nojiri M., Hishikawa Y., Togawa E., Romanovicz D., and Brown, Jr. R.M. 2002. Biodirected epitaxial nanodeposition of polymers on oriented macromolecular templates. Proc Natl Acad Sci USA 99:14008–14013.

Kondo T., Kasai W., and Brown, Jr. R.M. 2004. Formation of nematic ordered cellulose and chitin. Cellulose 11:463–474.

Langan P., Nishiyama Y., and Chanzy H. 1999. A revised structure and hydrogen bonding system in cellulose II from a neutron fiber diffraction analysis. J Am Chem Soc 121:9940–9946.

Minke R. and Blackwell J. 1978. The structure of α-chitin. J Mol Biol 120:167–181.

Togawa E. and Kondo T. 1999. Change of morphological properties in drawing water-swollen cellulose films prepared from organic solutions. a view of molecular orientation in the drawing process. J Polym Sci B: Polym Phys 37:451–459.

Thompson N.S., Kaustinen H.M., Carlson J.A., and Uhlin K.I. 1988. Tunnel structures in *Acetobacter xylinum*. Intl J Biol Macromol 10:126–127.

Whaley S.R., English D.S., Hu E.L., Barbara P.F., and Belcher A.M. 2000. Selection of peptides with semiconductor binding specificity for directed nanocrystal assembly. Nature 405:665–668.

Ward I.M. (ed.) 1997. Structure and Properties of Oriented Polymers. Chapman & Hall, London, p. 1.

Zhao X.-M., Whitesides G.M., Qin D., Xia Y., Rogers J.A., and Jackman R.J. 1998. Microfabrication, microstructures and microsystems. In Manz A. and Becker H. (eds.) Microsystem Technology in Chemistry and Life Sciences, Vol.194. Springer, Berlin, p. 1–20.